Korean J. Chem. Eng., 40(1), 195-204 (2023)
DOI: 10.1007/s11814-022-1245-6

pISSN: 0256-1115
eISSN: 1975-7220

Pervaporation performance of BTESE/TEOS-derived organosilica membrane and its stability in isopropanol aqueous solutions

Hongdan Wu*,,‡,†, Xiaodi Liu**, Xiaoyu Yang**, Chuanzhi Hu**, and Zhihui Zhou*,**,‡,†**

*Hubei Key Laboratory for Efficient Utilization and Agglomeration of Metallurgic Mineral Resources, Wuhan University of Science and Technology, Wuhan, Hubei 430081, China
**College of Resource and Environmental Engineering, Wuhan University of Science and Technology, Wuhan, Hubei 430081, China
(*Received 18 April 2022 • Revised 25 July 2022 • Accepted 29 July 2022*)

Abstract−Organosilica membranes derived from bis(triethoxysilyl)ethane (BTESE) and tetraethyl orthosilicate (TEOS) were prepared by sol-gel method on porous α-Al_2O_3 supports and applied in pervaporation dehydration of isopropanol (IPA) aqueous solutions. The permeation characteristics of membranes in IPA/water mixture were evaluated for preparation conditions and stability, including long-term stability, acid resistance, and feed concentration. It was observed that the water contact angle of BTESE/TEOS-derived organosilica membrane decreased from (77.74±0.47) ° to (36.67±1.05) ° as the content of TEOS increased, which proved that the surface property of the membrane could be changed by the part of hydrocarbon units after hydrolysis condensation reaction. As the molar ratio of BTESE to TEOS was 1 : 2, the organosilica membrane showed high pervaporation performance for 90 wt% isopropanol aqueous solutions at 75 °C, with a water permeation flux of 10.580 $kg \cdot m^{-2} \cdot h^{-1}$ and separation factor of 1170. Stability experiments of long-term operation and acid environment in isopropanol aqueous solutions showed slight changes in flux and separation factor, proving that organosilica membranes had better stability. An increase in IPA concentration from 60 wt% to 90 wt% decreased both water flux and water content on the permeate side, suggesting that the effective pore sizes for permeation could be reduced by adsorption of IPA molecules, whereas the membrane remained high permeance in isopropanol aqueous solutions with high water content. The separation mechanism of pervaporation dehydration of isopropanol aqueous solutions by BTESE/TEOS-derived membrane was mainly attributed to the molecular sieve separation effect. The results showed that the BTESE/TEOS-derived organosilica membranes had an application prospect in the dehydration of aqueous-organic mixtures.

Keywords: Organosilica Membrane, Pervaporation Dehydration, Stability, Isopropanol Aqueous Solutions

INTRODUCTION

Pervaporation (PV) is a well-known separation technique that can be used to dehydrate aqueous organic mixtures, remove traces of volatile organic compounds from aqueous solutions, and separate organic solvent mixtures, particularly azeotropic mixtures and mixtures with similar boiling points [1-3]. Over the past few decades, researchers have focused on the dehydration of aqueous-organic mixtures, mainly on ethanol aqueous and isopropanol (IPA) aqueous systems [4].

Inorganic membranes with high thermal and chemical durability, such as zeolite [5-8], carbon molecular sieve [9,10], and amorphous silica [11,12], have been used to dehydrate aqueous-organic mixtures. In particular, zeolite membranes have been successfully implemented for dehydration of alcohol/water solutions due to their high selectivity and permeability [8,13-16]. However, it has been reported that the destruction of basic framework structure of zeolite in acidic or high water content solutions could lead to a lower stability of membranes [17]. Therefore, stability in special working environment, such as acidic solutions, high water content dehydration systems, is one of the significant research focuses of membrane materials.

Due to their thermal stability and chemical resistance properties, amorphous silica and silica-based membranes prepared by sol-gel processing are acknowledged as promising pervaporation membranes [18-20]. Yang et al. prepared SiO_2-ZrO_2 amorphous silica membranes by sol-gel method and conducted experiments of dehydration of isopropanol aqueous solutions, with results of water flux as high as 2.16 $kg \cdot m^{-2} \cdot h^{-1}$ and separation factor over 10,000 at 75 °C [21]. Despite the fact that silica-based membranes performed well in terms of pervaporation, the instability of amorphous silica in aqueous-organic mixtures limits its application because silica will dissolve into water systems so that the morphology of silica will alter upon exposure to water environment, i.e., attributed to the collapse of small pores and expansion of larger pores, resulting in a loss of selectivity.

Several types of metal ions were doped into silica networks to improve the stability of silica-based membranes, thus reducing the hydrophilicity of silica. Boffa et al. [22] investigated the hydrothermal stability of microporous niobia-silica membranes, which were more stable under hydrothermal conditions than silica membranes

†To whom correspondence should be addressed.
E-mail: wu_dan725@wust.edu.cn, zhouzh_wust@163.com
‡These two authors contributed equally to this work.

due to hydrothermally stable Nb-O-Si bonds. Wang et al. [23] found cobalt-doping gave enhanced stability of silica membranes by up to 150 days in an aqueous mixture.

In addition, incorporation of hydrolytically stable groups can also improve the stability of silica-based membranes, such as hydrophobic functional groups. Nowadays, a novel form of organosilica membrane has been developed using bridging alkoxides such as bis(triethoxysilyl)ethane (BTESE) and methyltriethoxysilane (MTES), in which the hydrophobic functional groups shelter the siloxane linkages from water and make the membrane highly stable in aqueous environments [24-26]. Organosilica membranes derived from BTESE might be used to dehydrate aqueous solutions of ethanol, isopropanol, and acetic acid by pervaporation and vapor permeation. Wang et al. reported that BTESE-derived organosilica membrane with looser silica network formed by the bridged unit of the alkoxide showed a water flux of 2.5 $kg \cdot m^{-2} \cdot h^{-1}$ with a separation factor of 100 in PV dehydration of 90 wt% ethanol aqueous solutions at 75 °C [27]. BTESE membrane fired at 100 °C with HCl treatment to tune the silica network by reducing the pore size showed a water flux of 2.46 $kg \cdot m^{-2} \cdot h^{-1}$ and a separation factor of 3960 during the pervaporation dehydration of a 90 wt% isopropanol aqueous solutions at 75 °C [28]. A layered hybrid membrane using BTESE as a single precursor on a porous polysulfone support was applied to the vapor permeation dehydration of isopropanol-water (90/10 wt%) solutions at 105 °C, demonstrating a water flux of 1.6 $kg \cdot m^{-2} \cdot h^{-1}$ and a separation factor of 315 [29]. Tsuru et al. developed BTESE-derived membranes and reported that permeation flux of membrane for aqueous acetic acid (AcOH) solutions (AcOH: 90 wt%, 75 °C) was 2.0-4.0 $kg \cdot m^{-2} \cdot h^{-1}$ with water selectivity of 200-500 [30]. In our previous study, we reported that a BTESE-derived membrane on porous α-Al_2O_3 tubular support revealed a higher water content on the permeate side of 99.4% and an average water flux of 1 $kg \cdot m^{-2} \cdot h^{-1}$ for 15 wt% isopropanol aqueous solutions at 75 °C [31]. Hydrolytic condensation of BTESE could form a circular carbo siloxane structure, which could not form a continuous network structure with some co-condensation groups, thus affecting pore size and water permeation flux of membrane. The pore size of organosilica membranes can be controlled by the organic-inorganic hybrid silica network [24]. Herein, controlling pore size and silica network by mixing precursors derived from different alkoxides has been proposed. Castricum et al. [32] obtained a variety of silica materials with varying ratios of MTES and TEOS (tetraethoxysilane) and found that the ratio of precursors might effectively influence the pore and network structure of the material. Hence, to improve the pervaporation performance of silica membranes in aqueous systems, an organosilica membrane by mixing precursors of BTESE and TEOS was proposed to design. Meng et al. [33] prepared an organosilica membrane by mixing precursors of BTESE and TEOS for O_2/SO_2 gas separation, and Chai et al. [34] prepared organic-inorganic hybrid silica membranes with different ratios of BTESE and MTES for gas separation. As far as we know, no report can be found on BTESE/TEOS-derived organosilica membranes used for aqueous-organic mixtures separation.

In this work, in order to improve the water flux and stability, BTESE/TEOS-derived organosilica membranes were prepared by sol-gel method by mixing BTESE and TEOS as Si precursor, which were applied to the dehydration of isopropanol aqueous solutions. The effects of preparation conditions on structure and pervaporation performance for organosilica membranes were investigated. Moreover, long-term stability, acid resistance and feed concentrations were conducted on the membrane.

EXPERIMENTAL

1. Materials

The 1,2-bis(triethoxysilyl)ethane (BTESE) and Zirconium (IV) butoxide solution (ZrBT) were purchased from Aladdin Co., Ltd. (Shanghai, China). Tetraethoxysilane (TEOS) was purchased from Tianjin Baishi Chemical Industry Co., Ltd. (Tianjin, China). Isopropanol (IPA) and ethanol were purchased from Tianjin Beilian Fine Chemicals Development Co., Ltd. (Tianjin, China). Hydrochloric acid (HCl) and acetic acid (Ac) were purchased from Kunshan Jincheng Reagent Co., Ltd. (Jiangsu, China). All chemicals were of analytical grade and used without further purification. Deionized water was used throughout the study.

2. Preparation of Organosilica Sols and Membranes

Five types of sols were prepared with the molar ratios of BTESE to TEOS of 1/0 (pure BTESE), 1/1, 1/2, 1/3, and 0/1 (pure TEOS), respectively. The BTESE-TEOS organosilica sols were prepared by hydrolysis and polymerization reaction in ethanol solvent. First, deionized water and HCl were added in the ethanol. Then, a mixture of BTESE-TEOS organosilica sols was added dropwise to the solutions under intensely agitating at 60 °C with established ratios. All the solution was with molar ratios of $Si/H_2O/H^+=1:60:0.1$. After 90 min, the sol preparation process was quenched in an ice bath. Finally, a moderate amount of ethanol was added to keep equivalent weight of 5 wt% silane.

Organosilica membrane was fabricated on porous α-Al_2O_3 tubular supports with 2.5 μm pore size, 12 mm outside diameter and 100 mm length. Two types of α-alumina particles (1.9 μm and 0.2 μm) were coated on the support surface to fill major pinholes (SiO_2-ZrO_2 solution as a binder) and the support was fired at 550 °C each time to make a smooth mesoporous particle layer for an organosilica membrane. ZrTB and TEOS were hydrolyzed to 0.5 wt% SiO_2-ZrO_2 sol (Si/Zr=1/1), and then coated onto the particle layer. The membrane was fired under ambient air for 0.5 h at 550 °C to form an intermediate layer. Ultimately, BTESE-TEOS organosilica sols were deposited on the pretreated supports and membrane was fired at different temperature in ambient air for 1 h. The coating process was repeated several times to get total coverage. M-1/0, M-1/1, M-1/2, M-1/3, and M-0/1 were the names given to the corresponding hybrid membranes.

3. Characterization

The microstructure of the membrane layer was analyzed using Nova 400 Nano-SEM field emission scanning electron microscope of the US FEI company (working voltage 10 kV, working distance 5.9 mm, secondary electron imaging). To examine the functional groups, infrared (FT-IR) spectroscopic transmission spectra were acquired with a Nicolet spectrometer (Thermo Fisher) in the 4,000-300 cm^{-1} range. Using deionized water droplets to test water contact angle with evaluated through measurement device (Shanghai Zhongchen Tech) at indoor temperature. The adsorption isotherm

and pore size of powder were characterized by N_2 sorption at 77 K (ASAP 2020M, Micromeritics Co.).

4. PV Dehydration Experiments

PV dehydration experiments were carried out using a typical experimental apparatus equipped with thermostatic magnetic stirrer and a vacuum pump. All experiments were performed using isopropanol aqueous solutions at 75 °C. To provide a homogeneous solution, the feed IPA/water mixture was constantly cycled during the experiment. A vacuum pump was utilized to create negative pressure (1 mbar) for the entire scheme, allowing the vapors to be collected on the product side with the help of a nitrogen trap. Gas chromatography (GC9790, Zhejiang Fuli Co., Ltd) was used to measure feed and product concentrations, and the weight of condensate collected via the nitrogen trap at particular time intervals was used to calculate permeation flux. The separation factor and flux for newly manufactured membranes were then calculated by Eqs. (1) and (2).

$$J = \frac{M}{A \cdot t} \quad (1)$$

where J is the permeation flux ($kg \cdot m^{-2} \cdot h^{-1}$), M is weight of condensate (kg), A is the membrane area (m^2) and t is the operational time (h).

$$\alpha = \frac{Y_A / Y_B}{X_A / X_B} \quad (2)$$

where α is the separation factor, Y_A and Y_B are mass fractions of water and IPA (on the permeate side), whereas on the feed side, X_A and X_B are mass fractions of water and isopropanol aqueous solutions, respectively.

RESULTS AND DISCUSSION

1. The Formation of Amorphous Silica Networks

FT-IR analysis was used to determine the presence of organic moieties in silica networks, as summarized in Fig. 1. The gels derived from BTESE, BETSE-TEOS (molar ratio=1 : 2) and TEOS were fired in air at 300 °C for 1 h. A strong peak of Si-O bonding was observed around 1,070 cm^{-1} due to asymmetric stretching of oxygen atoms, while Si-O-Si peaks were observed at roughly 800 cm^{-1} due to symmetric stretching of oxygen atoms. These results indicated that the hydrolysis condensation reaction of silica gel prepared by different precursors was successful [35]. The peaks of Si-O bond (1,070 cm^{-1}) and Si-O-Si bond (800 cm^{-1}) shifted to lower wave numbers in BTESE and BTESE-TEOS sols were owing to an increasing of carbon content in organosilica networks. Absorption peaks of Si-OH group and adsorbed water appeared at 950 cm^{-1} and 3,750 cm^{-1}, respectively. When BTESE and BETSE-TEOS-derived silica gels were compared to the TEOS-derived silica gels, a new characteristic peak at 2,929 cm^{-1} ascribed to the stretching

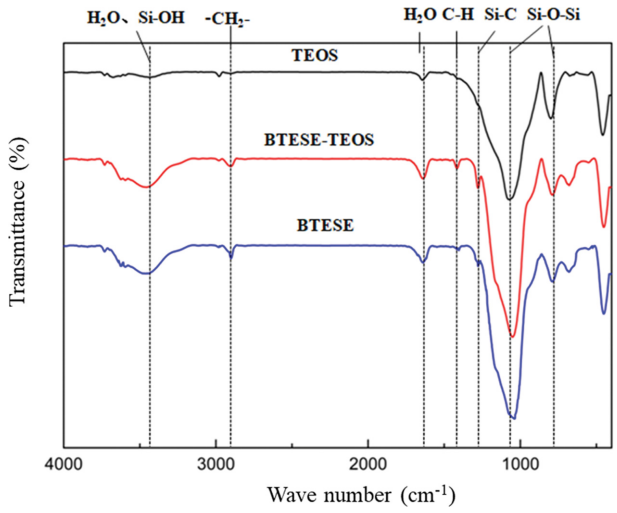

Fig. 1. FT-IR spectra on KBr plates of organosilica silica membranes derived from TEOS, BTESE and BETSE-TEOS.

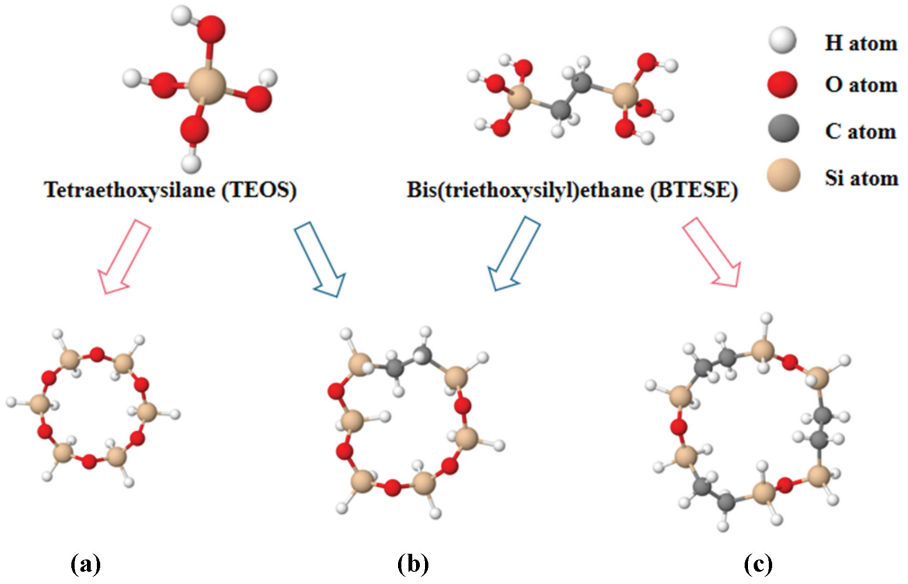

Fig. 2. Schematic diagrams of amorphous silica networks derived from TEOS (a), BTESE-TEOS (b) and BTESE (c).

vibrations of -CH_2- bonding in the Si-$(CH_2)_2$-Si group was observed; meanwhile, 1,340 cm^{-1} attributed to symmetric C-H stretching vibration in the -CH_2- fragments and 1,278 cm^{-1} attributed to the Si-C bond were clearly observed [36]. The presence of C-H bonds in BTESE/TEOS-derived silica network indicated that a partly cross-linked polysiloxane structure containing hydrocarbon units was formed by the cohydrolysis and condensation of BTESE with TEOS, according to the structure of the BTESE and TEOS precursors.

The schematic diagrams of amorphous silica networks derived from TEOS, BTESE-TEOS and BTESE are shown in Fig. 2. Amorphous silica derived from TEOS was formed as an Si-O-Si network by hydrolysis and condensation reactions. Because the organic groups between the Si atoms in the BTESE precursor were not hydrolyzed during the hydrolysis and polymerization, the Si-C-C-Si and Si-O-Si bonds coexisted in organosilica membranes derived from BTESE-TEOS. Therefore, the average pore size of silica network of BTESE-TEOS was between TEOS and BTESE, and the looser structure formed by BTESE-TEOS precursor would help to enhance the water flux of membrane.

2. Characterization of Organosilica Membrane

The surface and cross-sectional SEM images of BETSE/TEOS-derived organosilica membrane are shown in Fig. 3(a) and 3(c). There were no cracks or pinholes on the surface of membrane, indicating a continuous and compact surface. The cross-sectional image revealed three layers: the separation layer (BTESE-TEOS) and intermediate layer (SiO_2-ZrO_2), α-Al_2O_3 particles layer, α-Al_2O_3 support layer, respectively. The Al_2O_3 particles were used to modify the defects with large holes of the α-Al_2O_3 support, which the thickness was approximately 2.5 μm. SiO_2-ZrO_2 intermediate layer could further increase the adhesion between the layers and distribute the separation layer of colloidal particles uniformly. Separation layer for the BTESE/TEOS-derived organosilica membrane was successfully formed on the SiO_2-ZrO_2 intermediate layer. The intermediate and separation layers of the BTESE/TEOS-derived organosilica membrane were roughly 1 m thick and difficult to distinguish from one another.

The specific distribution of Si, Zr, C and O elements on the surface of the BETSE/TEOS-derived organosilica membrane was obtained by EDS analysis (Fig. 3(b) and 3(d)), which were distributed uniformly on the surface of the membrane. The O and Si elements were due to the introduction of both elements into the coating process of each layer. The Zr element exists because the binder (SiO_2-ZrO_2 sol) was coated during the preparation of the α-Al_2O_3 particles layer and the interlayer, while the element was not introduced into the separation layer. The Al element exists because of the coating of α-Al_2O_3 particles on the support layer. The C element exists only in the network structure of the separation layer, and its uniform distribution was due to the fact that the precursor of silicon dioxide sol, BTESE, contains-CH_2-groups, owing to uniformly present in the sol after sufficient hydrolysis and condensation reaction, thus indicating the homogeneity of the network structure of the silicon dioxide derived from BTESE-TEOS, which was necessary for the formation of high separation performance membranes.

3. PV Performance of Isopropanol Aqueous Solutions

The organosilica membranes prepared with different ratios of precursors were conducted to pervaporation experiments of isopropanol aqueous solutions (IPA, 90 wt%) at 75 °C, as shown in Fig. 4. When the precursor was only BTESE, the water flux of organosilica membrane was almost constant at 6.755 to 7.103 $kg \cdot m^{-2} \cdot$

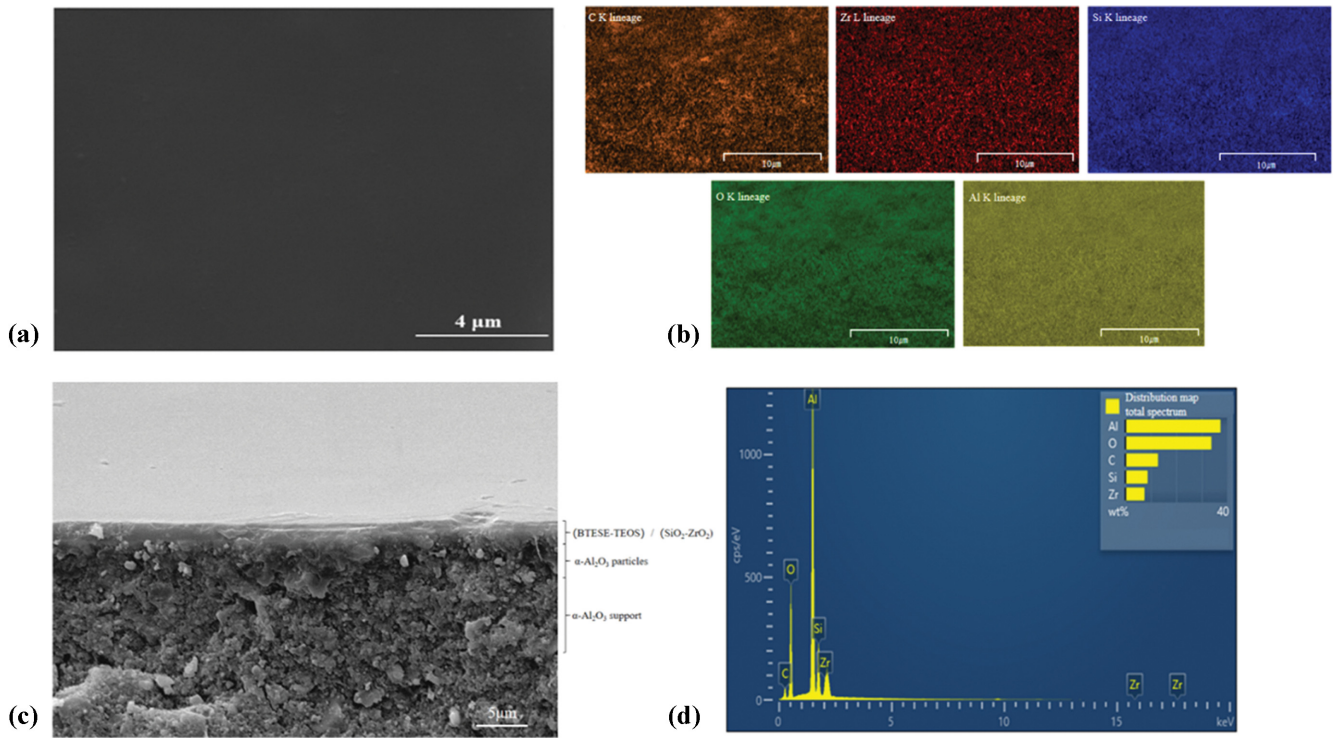

Fig. 3. The surface and cross-sectional SEM images and energy spectra images of BETSE/TEOS-derived organosilica membrane (M-1/2).

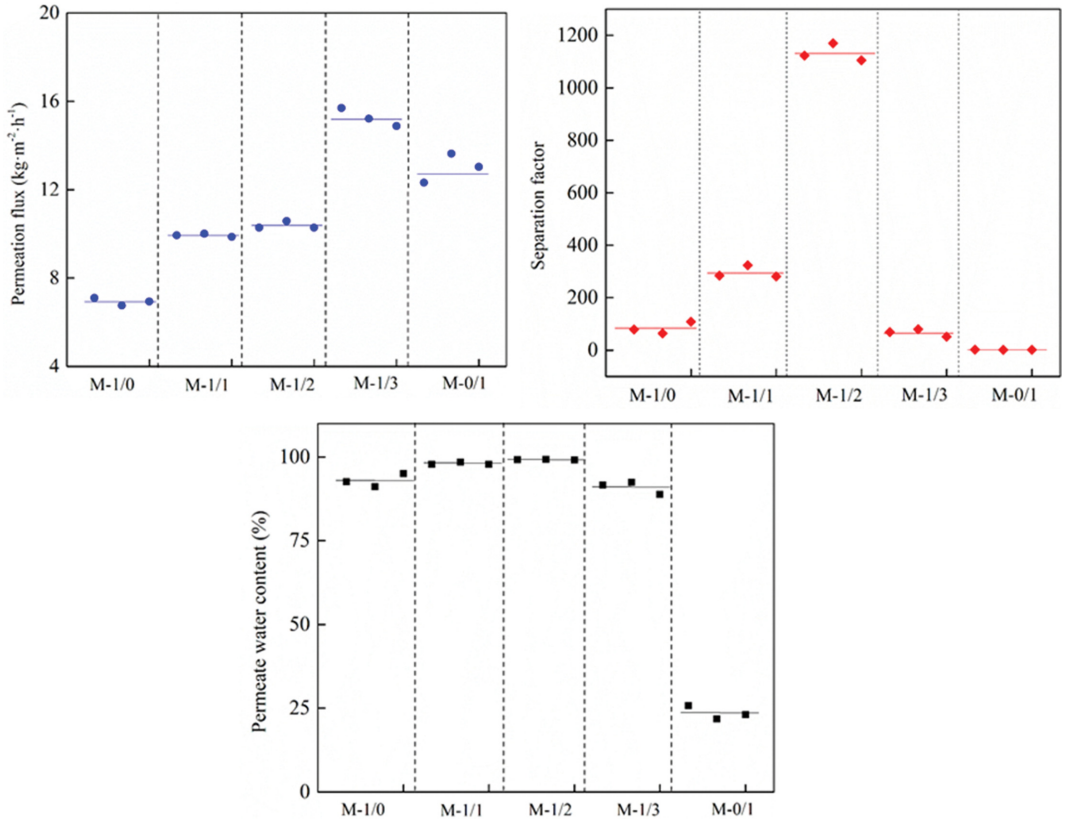

Fig. 4. PV performance of membranes with different ratios of precursors (IPA, 90 wt%, 75 °C).

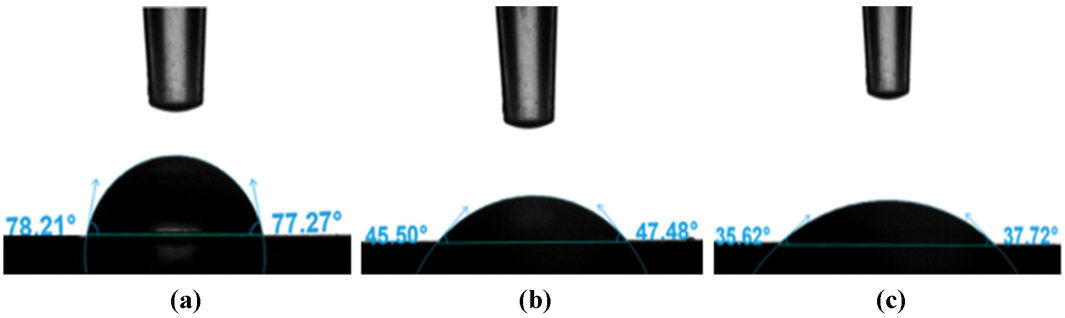

Fig. 5. Water contact angle of BTESE/TEOS-derived organosilica membranes with different ratios of precursors. (a) BTESE : TEOS=1 : 1, (b) BTESE : TEOS=1 : 2, (c) BTEST : TEOS=1 : 3.

h^{-1}, with a maximum separation factor only of 108. Organic hydrophobic groups in structure of BTESE could repel water molecules during pervaporation. Meanwhile, the BTESE had a self-condensation reaction in the process of reaction, in which a circular carbo siloxane structure was formed first and then condensed with other molecules (Fig. 2(c)), so that large pore size was easily formed by the silica networks, thus resulting in reducing the separation performance. The silica membrane prepared by TEOS as precursor has basically no separation effect in the dehydration process of isopropanol aqueous solutions at 75 °C, which was due to poor hydrothermal stability caused by Si-O-Si networks (Fig. 2(a)). When two precursors were introduced simultaneously, self-condensation reaction of BTESE could be inhibited (Fig. 2(b)); moreover, organic groups of BTESE could enhance the hydrothermal stability of silica composite, resulting in forming more homogeneous and dense networks, which was beneficial to pass though water. The BTESE/TEOS-derived membrane showed best PV performance for 90 wt% isopropanol aqueous solutions at 75 °C as the molar ratio of BTESE to TEOS was 1 : 2, namely the permeate flux was 10.580 kg/(m^2 h) and the water content water content on the permeate side was 99.248% with separation factor of 1170, respectively.

Furthermore, BTESE/TEOS-derived organosilica membranes prepared with different ratios of precursors showed different surface properties, such as hydrophilic or hydrophobic, which could affect the separation performance for isopropanol aqueous solutions to a certain extent. To clarify this point, measurements of water contact angle were carried out, as shown in Fig. 5. In the preparation process of silica sol, the silica networks were changed due to the

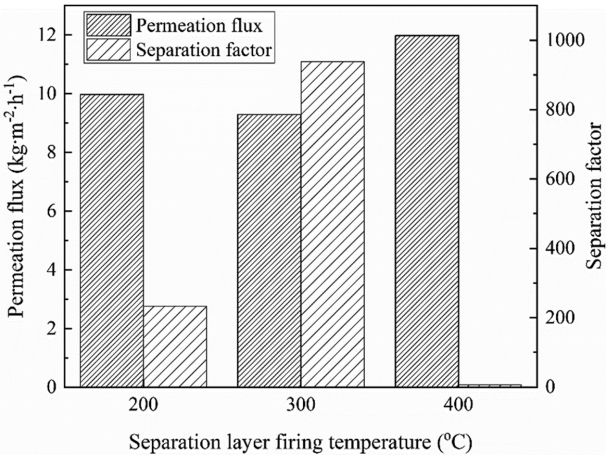

Fig. 6. PV performance of BTESE/TEOS-derived membrane separation layer firing at different temperature (IPA: 90 wt%, 75 °C).

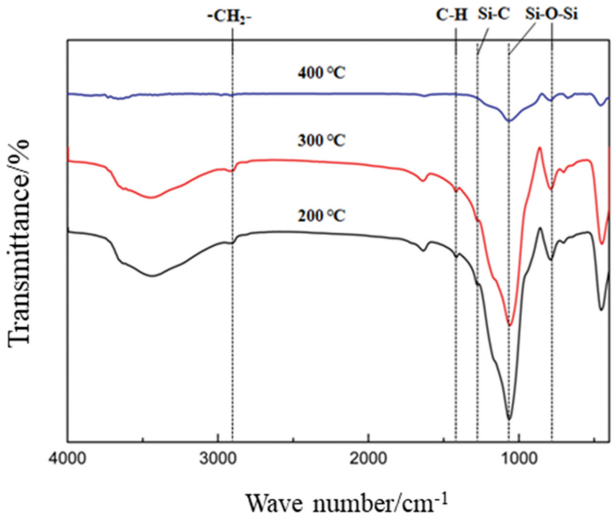

Fig. 7. FT-IR spectra of separation layer gels calcined at different temperature.

introduction of BTESE and TEOS, which led to the hydrophilicity and hydrophobicity of membrane changing. The contact angle decreased from (77.74±0.47)° to (36.67±1.05)° as the content of TEOS increased. It could be deduced following the structure of the precursors that hydrophobicity was caused by the part of hydrocarbon units (i.e., -CH_2- organic skeleton) after hydrolysis condensation reaction. As the molar ratio of BTESE to TEOS was 1 : 1, the water contact angle was lager with a higher content of BTESE, repulsive interaction of water molecules by hydrophobic groups would affect the separation effect. Although the hydrophilicity of membrane was best as the molar ratio of BTESE to TEOS was 1 : 3, due to the high content of TEOS, the main molecules involved in the hydrolysis condensation reaction were still TEOS with poor hydrothermal stability.

Most microporous silica membranes were prepared by firing at different temperature to form a loose silica structure [37,38]. Hence, the firing temperature of the separation layer was critical for producing silica membranes with high flux and acceptable separation performance. PV performance of BTESE/TEOS-derived membrane separation layer firing at different temperature for 1 h is shown in Fig. 6. With increasing separation layer firing temperature from 200 °C to 300 °C, the separation factor rose dramatically from 234 to 939, the water flux fell just marginally from 9.966 to 9.283 kg·m^{-2}·h^{-1}. Because the silica network densified at higher firing temperatures, the pores for IPA penetration shrank. However, when the firing temperature reached 400 °C, the separation factor was only 7, which showed the membrane had no separation effect. The higher temperature could cause the carbonization of organic groups and destroy the original silica network structure. Hence, the separation layer calcination temperature could change the network structure of the silica membranes.

The separation layer gels calcined at different temperature were tested by FT-IR analysis, as shown in Fig. 7. At 200 °C and 300 °C, the characteristic peaks with wave numbers of 2,929 cm^{-1}, 1,340 cm^{-1} and 1,278 cm^{-1}, which were generated by the stretching vibrations of -CH_2- bonding in the Si-$(CH_2)_2$-Si groups and symmetric C-H stretching vibration in the -CH_2- fragments and the existence of Si-C bond, were all observed obviously. However, the structural units containing C elements almost disappeared at 400 °C, prov-

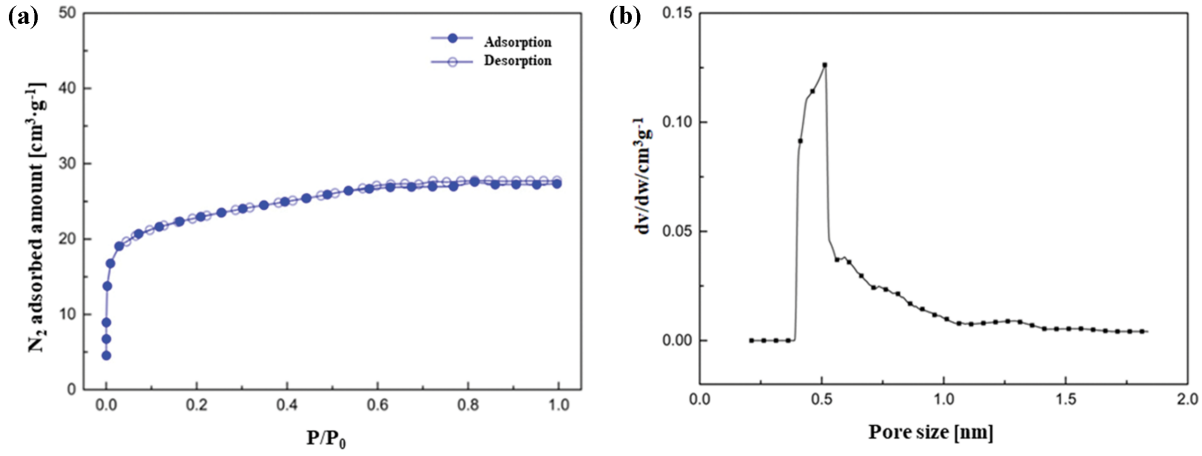

Fig. 8. (a) Nitrogen adsorption/desorption isotherms of as-prepared powders of sol power at 77 K (b) micropore analysis of silica membrane.

ing the carbonization phenomenon of BTESE/TEOS-derived membrane, resulting in no separation effect of membrane.

Pore size and distribution of silica sol powder were tested to further investigate the separation mechanism of BTESE/TEOS-derived membranes when the molar ratio of BTESE to TEOS was 1 : 2. Fig. 8(a) shows the N_2 adsorption/desorption isotherms of the sol powder. During the desorption process, the adsorption rate was relatively high in the low pressure range ($10^{-5}<P/P_0<0.05$), while there was no obvious hysteresis phenomenon in the high pressure range. The sol powder showed a type I isotherm curve, which corresponds to micropores.

H-K micropore analysis mode was further used to conduct mi-

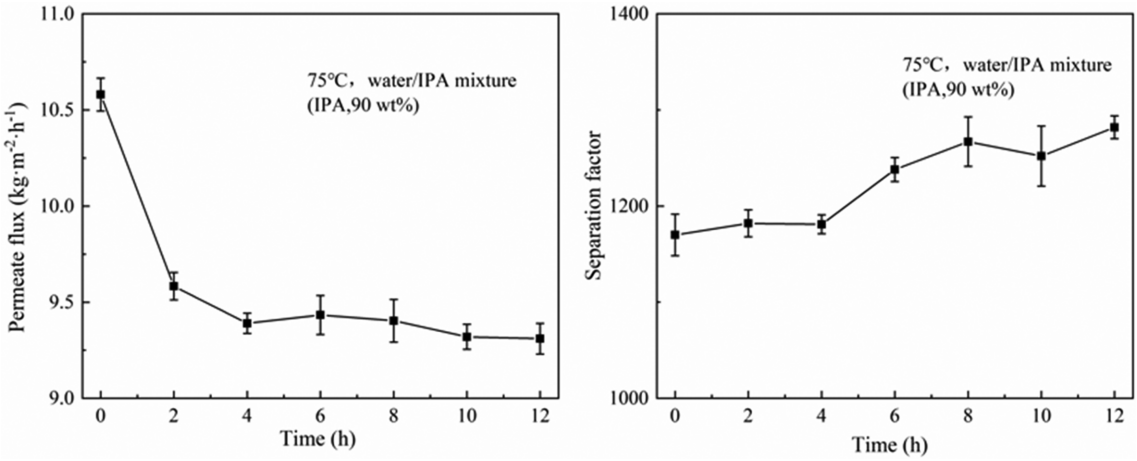

Fig. 9. Long-time course of PV performance for a water/IPA mixture (M-1/2, IPA, 90 wt%, 75 °C).

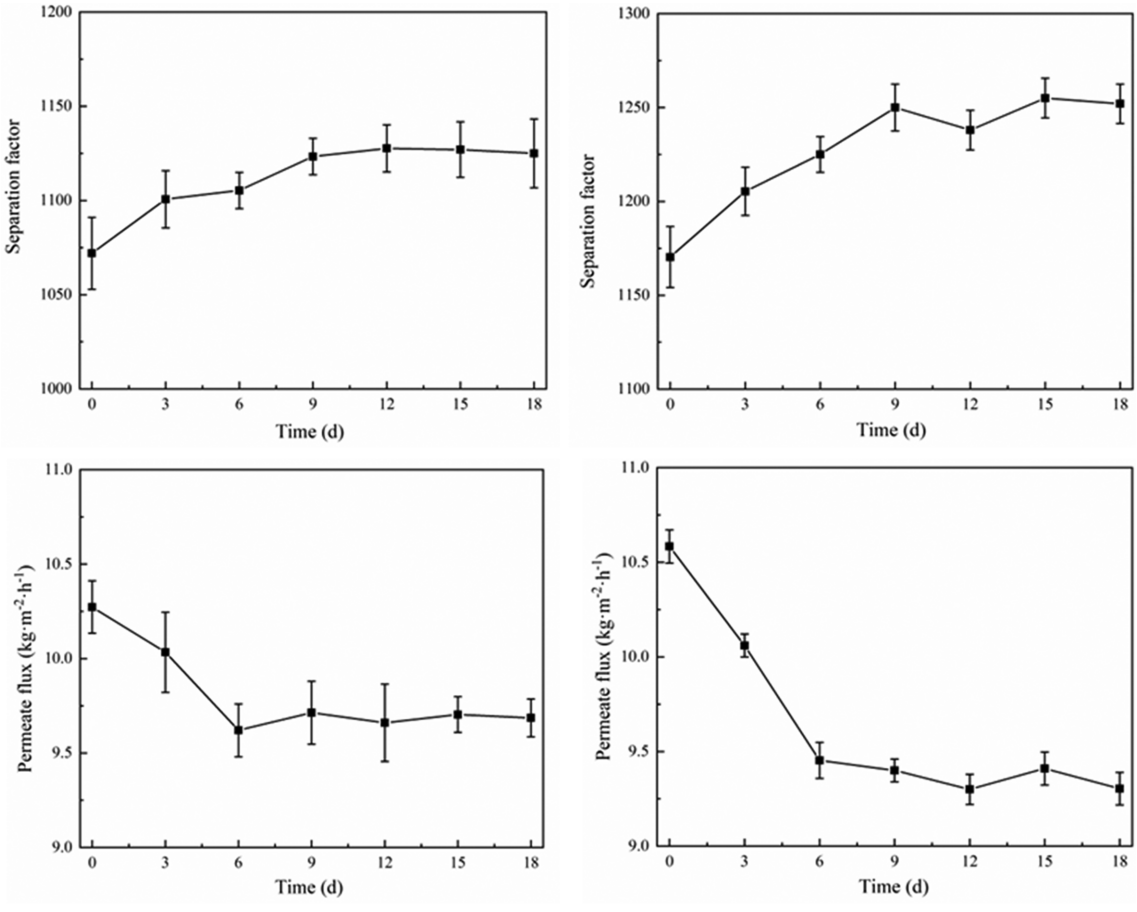

Fig. 10. PV performance of membrane after immersing in acid for a water/IPA mixture (M-1/2, IPA, 90 wt%, 75 °C), (a) Immersion in hydrochloric acid, (b) Immersion in acetic acid.

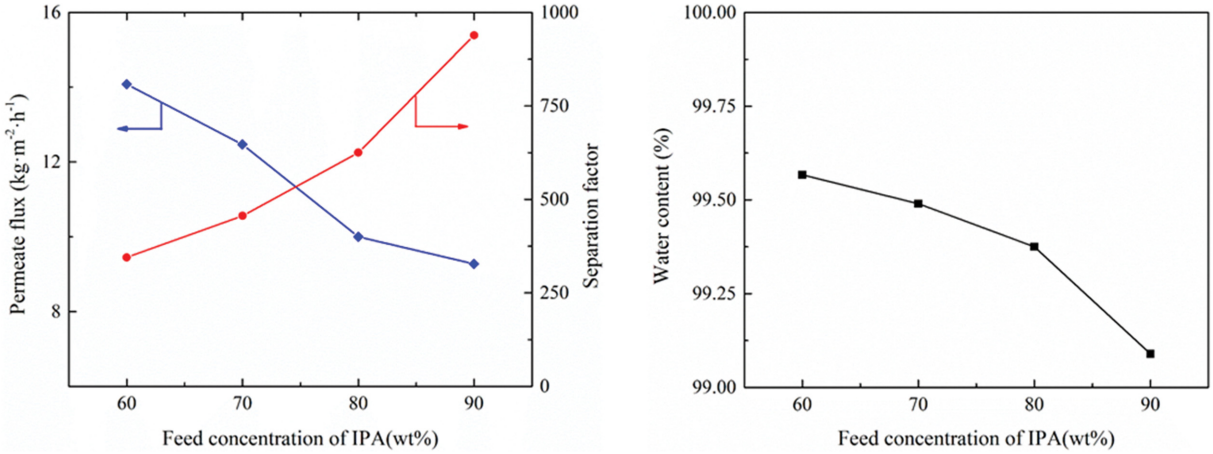

Fig. 11. Concentration dependency of PV performance for water/IPA mixture (M-1/2, 75 °C).

cropore analysis on silica materials, as shown in Fig. 8(b). The pore size distribution was concentrated at about 0.5 nm, and the average pore size was 0.518 nm. As we all know, the kinetic diameters of water molecule and isopropanol molecule were 0.265 nm and 0.58 nm, respectively. The separation mechanism of BTESE/TEOS-derived membrane could be identified as dominated by molecular sieve separation effect. Because the micropores formed by BTESE and TEOS were between water molecules and isopropanol molecules, smaller water molecules could pass through the membrane, while larger isopropanol molecules were trapped during pervaporation, thus a sieving effect of membrane.

4. Stability of BTESE/TEOS-derived Organosilica Membrane

The organosilica membrane showed a permeation flux more than 9 $kg \cdot m^{-2} \cdot h^{-1}$ and a separation factor >1,100 over the long operational time for a water/IPA mixture (IPA: 90 wt%) at 75 °C, as shown in Fig. 9. PV performance was relatively stable after a slight change over several hours, in which a tendency showed a decrease in water flux and a slight increase in the separation factor for the first 2 h, which was explained by the adsorption of IPA that reduced the pore sizes of membrane. Physical adsorption could reduce the average effective pore size and increase the separation factor. With the prolonging of pervaporation time, the molecules adsorbed on the existing pores basically reached the maximum value after continuous operation for 2 h, then the permeation flux and separation factor tended to be stable. The hydrophobic group of the BTESE precursor was shown to be responsible for rather constant PV performance, as evidenced by water contact angle measurements (Fig. 5).

Fig. 10 shows the time course of a water/IPA mixture (IPA: 90 wt%) at 75 °C by membrane M-1/2, in which membrane was immersed in hydrochloric acid and acetic acid at pH=2 for different times. Water flux was originally 10.277 $kg \cdot m^{-2} \cdot h^{-1}$ after immersion in hydrochloric acid and gradually declined to roughly 9.6 $kg \cdot m^{-2} \cdot h^{-1}$, while the separation factor remained relatively constant at 1125 from 1072. Meanwhile, water flux was gradually decreased from initially 10.580 $kg \cdot m^{-2} \cdot h^{-1}$ to stability at 9.3 $kg \cdot m^{-2} \cdot h^{-1}$ after immersion in acetic acid, and separation factor change from 1170 to 1250 in approximate equilibrium.

Furthermore, the performance changes could be ascribed to condensation reaction of the amorphous silica networks derived by BTESE and TEOS further occurring. During the preparation of sol, a small amount of hydrochloric acid would be introduced as a catalyst. The separation layer was formed by BTESE-TEOS calcination curing at 300 °C, resulting an incomplete condensation in some areas of the membrane. A few hydroxyl groups in the amorphous silica networks could react with other uncondensed hydroxyl groups, forming a Si-O-Si structure and resulting a dense membrane. Membrane M-1/2, after immersing in acid for 18 days and then used for dehydration of isopropanol aqueous solutions, also showed a stable flux and a high separation factor.

Fig. 11 shows concentration dependency in the range of 60-90 wt% of IPA. Due to the decreasing partial pressure of the water vapor, the water flux and water content on the permeate side decreased monotonically as the IPA concentration increased, in which the water flux decreased from 14.080 $kg \cdot m^{-2} \cdot h^{-1}$ to 9.277 $kg \cdot m^{-2} \cdot h^{-1}$, and the water content on the permeate side decreased from 99.567% to 99.089%, indicating hydrothermal stability of the membrane in isopropanol aqueous solutions with high water content. Water permeance reduced as a result, and separation factors increased from 345 to 939. As mentioned, the separation mechanism of pervaporation dehydration by BTESE/TEOS-derived membrane was mainly attributed to molecular sieve separation effect. As the separation process progressed, IPA molecules could not pass through the amorphous silica networks and were likely rejected on the surface, blocking water and IPA passing through. With increasing IPA concentration, more IPA molecules could adsorb on the outer surface of membranes, reducing the effective pore area for water to pass through. As a result, water and IPA permeance decreased. Because IPA is a larger molecule than water, the lower permeance for large molecules was more prominent, and water could pass through the membrane with no resistance, resulting in a higher separation factor. The PV performance data shown in Fig. 11 indicate the BTESE-TEOS-derived membrane can be used in the application of organic solutions pervaporation dehydration with high water content.

The PV performance of the BTESE/TEOS-derived organosilica membrane was compared to that of BTESE-derived membranes, zeolite membranes and mordenite membranes in Fig. 12. Generally speaking, BTESE-derived membranes showed moderate permeances and separation factors, while zeolite membranes showed

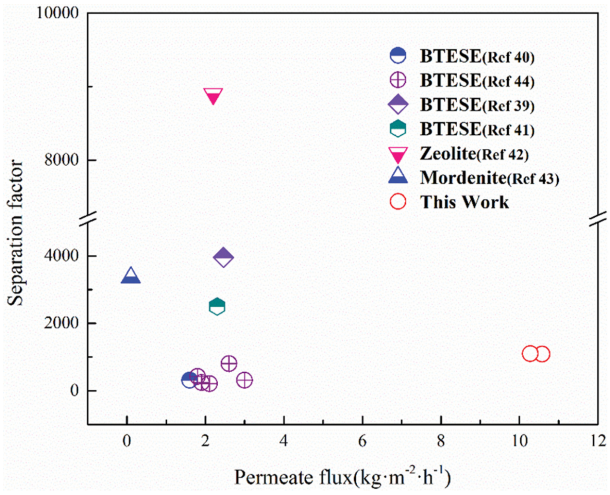

Fig. 12. PV performance of BTESE/TEOS-derived organosilica membrane compared with other reported membranes.

high separation factors with moderate permeances, mordenite membranes showed rather low permeance and moderate separation factors. In this work, BTESE/TEOS-derived organosilica membranes showed relatively high permeance and moderate separation factors, with the water flux more than 10 $kg \cdot m^{-2} \cdot h^{-1}$ for 90 wt% isopropanol aqueous solutions and a separation factor >1,100.

Compared to inorganic membranes (zeolite and mordenite membranes), although the separation factor was not as high, BTESE/TEOS-derived organosilica membranes exhibited an excellent high permeation flux, which was due to the thickness and pore size of the derived membranes being more suitable for water molecules to pass through, thus increasing the permeation flux. In contrast to BTESE-derived membranes, the pore size of BTESE/TEOS-derived organosilica membranes could be effectively controlled by mixing precursors of BTESE and TEOS, which was beneficial to the improvement of permeation flux.

Meanwhile, BTESE-TEOS-derived organosilica membranes showed quite stable PV performance in IPA/water mixtures, leading to the conclusion that BTESE-TEOS-derived organosilica membranes are a viable candidate for pervaporation dehydration of organic solvents.

CONCLUSIONS

Organosilica membranes derived from BTESE and TEOS were produced using the sol-gel method on porous α-Al_2O_3 supports and applied in pervaporation dehydration of isopropanol aqueous solutions. As the molar ratio of BTESE to TEOS was 1 : 2, the water permeation flux for 90 wt% isopropanol aqueous solutions was 10.580 $kg \cdot m^{-2} \cdot h^{-1}$ at 75 °C with separation factor of 1170. The water contact angle of BTESE/TEOS-derived organosilica membranes decreased from (77.74±0.47)° to (36.67±1.05)° as the content of TEOS increased, which proved that the surface property of membrane could be changed by the part of hydrocarbon units after hydrolysis condensation reaction. The stability test in isopropanol aqueous solutions demonstrated that BTESE/TEOS-derived membranes had slight changes in flux and separation factors for long-term operation in an acidic environment, confirming better stability of organosilica membranes. An increase in IPA concentration from 60 wt% to 90 wt% decreased both water flux and water content on the permeate side, suggesting that adsorbed IPA on membranes reduced the effective pore sizes for permeation of the large molecules, whereas the membrane remained high permeance in isopropanol aqueous solutions with high water content. The separation mechanism of pervaporation dehydration by BTESE/TEOS-derived membrane was mainly attributed to molecular sieve separation effect.

The results reveal the great promise of BTESE/TEOS-derived organosilica membranes for separation applications, in which potential applications of the membranes would include the dehydration of aqueous-organic mixtures such as water/alcohol and water/isopropanol. Further study on membrane fabrication, including reducing multiple coating and coating on other supports, and long-term stability under membrane reactor conditions, will be important for industrial applications of BTESE/TEOS-derived organosilica membranes.

ACKNOWLEDGEMENTS

This work was supported by the Guiding Project of Science and Technology Research of Education Department of Hubei Province (Grant number B2020019).

REFERENCES

1. B. Smitha, D. Suhanya, S. Sridhar and M. Ramakrishna, *J. Membr. Sci.*, **241**, 1 (2004).
2. X. Cheng, F. Pan, M. Wang, W. Li and Z. Jiang, *J. Membr. Sci.*, **541**, 329 (2017).
3. M. T. Ravanchi, T. Kaghazchi and A. Kargari, *Desalination*, **235**, 199 (2009).
4. P. D. Chapman, T. Oliveira, A. G. Livingston and K. Li, *J. Membr. Sci.*, **318**, 5 (2008).
5. H. Kita, K. Horii, Y. Ohtoshi, K. Tanaka and K. I. Okamoto, *J. Mater. Sci.*, **14**, 206 (1995).
6. Y. Morigami, M. Kondo, J. Abe, H. Kita and K. Okamoto, *Sep. Purif. Technol.*, **25**, 251 (2001).
7. K. Kissick, A. Ghorpade and R. Hannah, *J. Membr. Sci.*, **179**, 185 (2000).
8. K. Sato, K. Sugimoto and T. Nakane, *J. Membr. Sci.*, **307**, 181 (2008).
9. Y. R. Dong, M. Nakao, N. Nishiyama, Y. Egashira and K. Ueyama, *Sep. Purif. Technol.*, **73**, 2 (2010).
10. S. Tanaka, T. Yasuda, Y. Katayama and Y. Miyake, *J. Membr. Sci.*, **379**, 52 (2011).
11. S. Kitao and M. Asaeda, *J. Chem. Eng. Jpn.*, **23**, 367 (1990).
12. H. Veen, Y. Delft, C. Engelen and P. Pex, *Sep. Purif. Technol.*, **22**, 361 (2001).
13. C. Ying, H. Kita and K. I. Okamoto, *J. Membr. Sci.*, **236**, 17 (2004).
14. X. Lin, E. Kikuchi and M. Matsukata, *Chem. Commun.*, **11**, 957 (2000).
15. G. Li, E. Kikuchi and M. Matsukata, *Sep. Purif. Technol.*, **32**, 199 (2003).
16. Y. Hasegawa, H. Hotta, K. Sato, T. Nagase and F. Mizukami, *J.*

Membr. Sci., **34**, 193 (2010).
17. Y. Hasegawa, T. Nagase, Y. Kiyozumi, T. Hanaoka and F. Mizukami, *J. Membr. Sci.*, **349**, 189 (2010).
18. M. Asaeda, Y. Sakou, J. Yang and K. Shimasaki, *J. Membr. Sci.*, **209**, 163 (2002).
19. M. Asaeda, M. Ishida and Y. Tasaka, *Sep. Purif. Technol.*, **40**, 239 (2005).
20. S. Sommer and T. Melin, *Chem. Eng. Process.*, **44**, 1138 (2005).
21. T. Yoshioka, T. Tsuru and M. Asaeda, *J. Membr. Sci.*, **284**, 205 (2006).
22. V. Boffa, D. Blank and J. Elshof, *J. Membr. Sci.*, **319**, 256 (2008).
23. J. Wang and T. Tsuru, *J. Membr. Sci.*, **369**, 13 (2011).
24. H. L. Castricum, A. Sah, R. Kreiter, D. Blank, J. F. Vente, T. Elshof and Johan, *J. Mater. Chem.*, **18**, 2150 (2008).
25. H. L. Castricum, R. Kreiter, H. Veen, D. Blank, J. F. Vente and T. Elshof, *J. Membr. Sci.*, **324**, 111 (2008).
26. M. Kanezashi, K. Yada, T. Yoshioka and T. Tsuru, *J. Am. Chem. Soc.*, **131**, 414 (2009).
27. J. Wang, M Kanezashi, T. Yoshioka and T. Tsuru, *J. Membr. Sci.*, **415**, 810 (2012).
28. J. Wang, G. Gong, M. Kanezashi, T. Yoshioka, K. Ito and T. Tsuru, *J. Membr. Sci.*, **441**, 120 (2013).
29. G. Gang, J. Wang, H. Nagasawa, T. Yoshioka and T. Tsuru, *J. Membr. Sci.*, **464**, 140 (2014).
30. T. Tsuru, T. Shibata, J. Wang, H. Ryeon, M. kanezashi and T. Yoshioka, *J. Membr. Sci.*, **25**, 421 (2012).
31. H. D. Wu, H. R. Liu and X. Y. Liu, *J. Chin. Ceram. Soc.*, **4**, 7 (2020).
32. H. L. Castricum, A. Sah, M. C. Mittelmeijer-Hazeleger, C. Huiskes and J. E. Elshof, [J]. *J. Mater. Chem.*, **17**, 1509 (2007).
33. L. Meng, M. Kanezashi, J. Wang and T. Tsuru, *J. Membr. Sci.*, **496**, 211 (2015).
34. S. H. Chai, H. B. Du, Y. Y. Zhao, Y. C. Lin, C. L. Kong and L. Chen, *Sep. Purif. Technol.*, **222**, 162 (2019).
35. C. H. Lo, M. H. Lin, K. S. Liao, M. D. Guzman, H. A. Tsai, V. Rouessac, T. C. Wei, K. R. Lee and J. Y. Lai, *J. Membr. Sci.*, **365**, 418 (2010).
36. J. H. Kim and Y. M. Lee, *J. Membr. Sci.*, **193**, 209 (2001).
37. R. Vos and H. Verweij, *Science*, **279**, 1710 (1998).
38. R. Vos and H. Verweij, *J. Membr. Sci.*, **143**, 37 (1998).
39. J. Wang, G. Gong, M. Kanezashi, T. Yoshioka, K. Ito annd T. Tsuru, *J. Membr. Sci.*, **441**, 120 (2013).
40. G. Gong, H. Wang, H. Nagasawa, M. Kanezashi, T. Yoshioka and T. Tsuru, *J. Membr. Sci.*, **464**, 140 (2014).
41. G. Gong, H. Wang, H. Nagasawa, M. Kanezashi, T. Yoshioka and T. Tsuru, *J. Membr. Sci.*, **472**, 19 (2014).
42. Y. Cui, H. Kita and K. Okamoto, *J. Membr. Sci.*, **236**, 17 (2004).
43. X. Lin, E. Kikuchi and M. Matsukata, *Chem. Commun.*, **11**, 957 (2000).
44. H. Nagasawa, N. Matsuda, M. Kanezashi and T. Tsuru, *J. Membr. Sci.*, **498**, 336 (2016).